Polyoxometalate-HKUST-1 composite derived nanostructured Na-Cu-Mo$_2$C catalyst for efficient reverse water gas shift reaction

Gaje Singh [a,d], Satyajit Panda [a,d], Siddharth Sapan [a], Jogender Singh [a], Pranay Rajendra

Chandewar [c], Ankush Biradar [b,d], Debaprasad Shee [c], Ankur Bordoloi [a,d,*]

a.   Light and Stock Processing Division, CSIR-Indian Institute of Petroleum (IIP),

Dehradun-248005, India

b.   Inorganic Materials and Catalysis Division, CSIR-Central Salt and Marine Chemicals

Research Institute, G. B. Marg, Bhavnagar-364002, India

c.   Department of Chemical Engineering, Indian Institute of Technology, Hyderabad

502284, India

d.   Academy of Scientific and Innovative Research (AcSIR), Ghaziabad-201002, India

*Corresponding author: Light and Stock Processing Division, CSIR-Indian Institute of

Petroleum (IIP), Dehradun 248005, India.

*Corresponding author. E-mail address: ankurb@iip.res.in (A. Bordoloi)

Experimental Details

Catalyst characterizations

The PROTO AXRD® Benchtop Powder diffractometer, equipped with a NaI (Tl) scintillation counter detector and CuKα radiation (0.154 nm), was used to capture X-ray diffraction (XRD) patterns from 10 to 80°. The samples were measured At room temperature using an X-ray power of 600 Watts (40 kV/15 mA). The Scherrer equation determined the crystalline size of the catalysts,

$$d = \frac{K\,\lambda}{\beta \cos\theta}$$

Where d is crystalline size, K is the Scherrer constant (0.9), λ is the wavelength of the X-ray beam used (0.154 nm), β is the Full width at half maximum (FWHM) of the peak, and θ is the Bragg angle.

A Horiba LabRAM HR Evolution Raman Spectrometer was used to acquire Raman spectra with a 532 nm laser serving as the excitation source. Before analysis, the apparatus's synapse detector was thermoelectrically cooled to -75 °C, and the x-axis of the instrument was calibrated using a silicon wafer.

A tungsten filament doped with lanthanum hexaboride (LaB6) and a high vacuum ETD detector was used to capture SEM pictures of the synthesized catalyst using an FEI Quanta 200 F. The analysis was conducted by spreading the samples out on carbon tape.

The JEOL JEM-2100 device was used to collect images for transmission electron microscopy (TEM) and high-resolution transmission electron microscopy (HR-TEM). For 30 min, a small amount of catalyst was sonicated and distributed throughout ethanol. The sample was then dried in a vacuum desiccator after a few drops were placed on a copper grid supported with lacey carbon. The grid was placed on the sample holder and the instrument's accelerating voltage was set to 160 kV before the analysis. The samples were next examined with a JEM-2100 electron microscope for a range of studies, such as energy-dispersive X-ray spectroscopy (EDS) mapping, HR-TEM images, TEM, and selected area electron diffraction (SAED) pattern.

The Inductively coupled plasma optical emission spectrometry (ICP-OES) was performed using the Teledyne Leeman Labs Prodigy7 instrument. A high-temperature argon plasma was used to ignite the atoms in a 20 ml aliquot, resulting in emission lines. The emission line intensity is compared to the intensity of the known and variable amounts of elements to calculate their concentration.

The CO_2 Temperature-Programmed Desorption (CO_2 TPD) analysis was performed using a Micrometrics® Autochem II 2920 instrument. An amount of 0.055 g of catalyst sample was placed in a U-shaped quartz reactor. The catalyst was pre-treated for 1 h at 200 °C in 25 ml.min^{-1} of He flow and then cooled to 50 °C. Subsequently, for CO_2 adsorption, a 40 ml.min^{-1} flow of 10 vol. % CO_2/He mixture gas was introduced into the reactor. Following that, the sample was exposed to 40 ml.min^{-1} He flows for 60 min to eliminate physisorbed species. The desorption was investigated using a 5 °C.min^{-1} ramping rate from 50 to 850 °C.

X-ray photoelectron spectroscopy (XPS) was performed using a Thermo Scientific NEXSA XPS spectrometer and monochromatic X-ray radiation (AlKα) (1486.6 eV) at a 15kV accelerating voltage. The calibration benchmark for all elemental binding energies was the adventitious C 1s peak at 284.8 eV. The Shirley-type background removal was used using the XPSPEAK41 software to fit the XPS spectra.

TGA was performed using a Perkin Elmer TGA 4000 Thermogravimetric Analyzer. A sample of approximately 5 mg was put in a ceramic sample pan. The samples were heated from 30°C to 800°C using a 20 ml.min^{-1} nitrogen flow at a ramp rate of 10°C/min.

The instrument used for Fourier transform infrared spectroscopy was made by Perkin Elmer Inc. in Massachusetts, USA. The apparatus was calibrated using the polystyrene calibration film. The samples were produced in moisture-free KBr pellets, and after that, pelletized specimens were analyzed with a deuterated triglycine sulfate (DTGS) detector with 4 cm^{-1} spectral resolution and accumulations of 8 spectra per scan in the infrared region from 4000 cm^{-1} to 400 cm^{-1}.

The N_2O titration study was also performed in the Micrometrics® Autochem II 2920 apparatus, and the quantity of H_2 Consumed following the N_2O titration was used to estimate the Cu metal dispersion (Dis_{Cu}) in the catalysts. A He flow was applied to 0.05 g of catalyst samples at 100 °C for 2 h. After that, the gas was changed to a flow of N_2O to oxidize the Cu metallic particles on the surface to Cu^+, and the process was continued for 2 h. The He flow was introduced to remove N_2O species that were remaining at the surface. A reduction by H_2 pulse reduction of exposed Cu_2O was then carried out at 350 °C, and the amount of H_2 consumed was measured.

Diffuse reflectance infrared Fourier transform (DRIFT) spectra were acquired with the Bruker Tensor 37 apparatus to explore intermediates and products in reactions. The DRFIT Cell (Praying MantisTM High-temperature reactor cell) was filled with around 0.05 g of catalyst and heated to 550 °C using a 10 ml/min N_2 flow. Subsequently, the flow was changed to 5 ml/min of CO_2 and 20 ml/min of H_2 at ambient pressure. The spectra were collected after 60 min, 120 min, 180 min, and 240 min of the reaction.

Element	Wt %	At %
C K	55.26	71.78
O K	24.93	24.31
P K	00.43	00.22
MoL	12.83	02.09
CuK	06.55	01.61
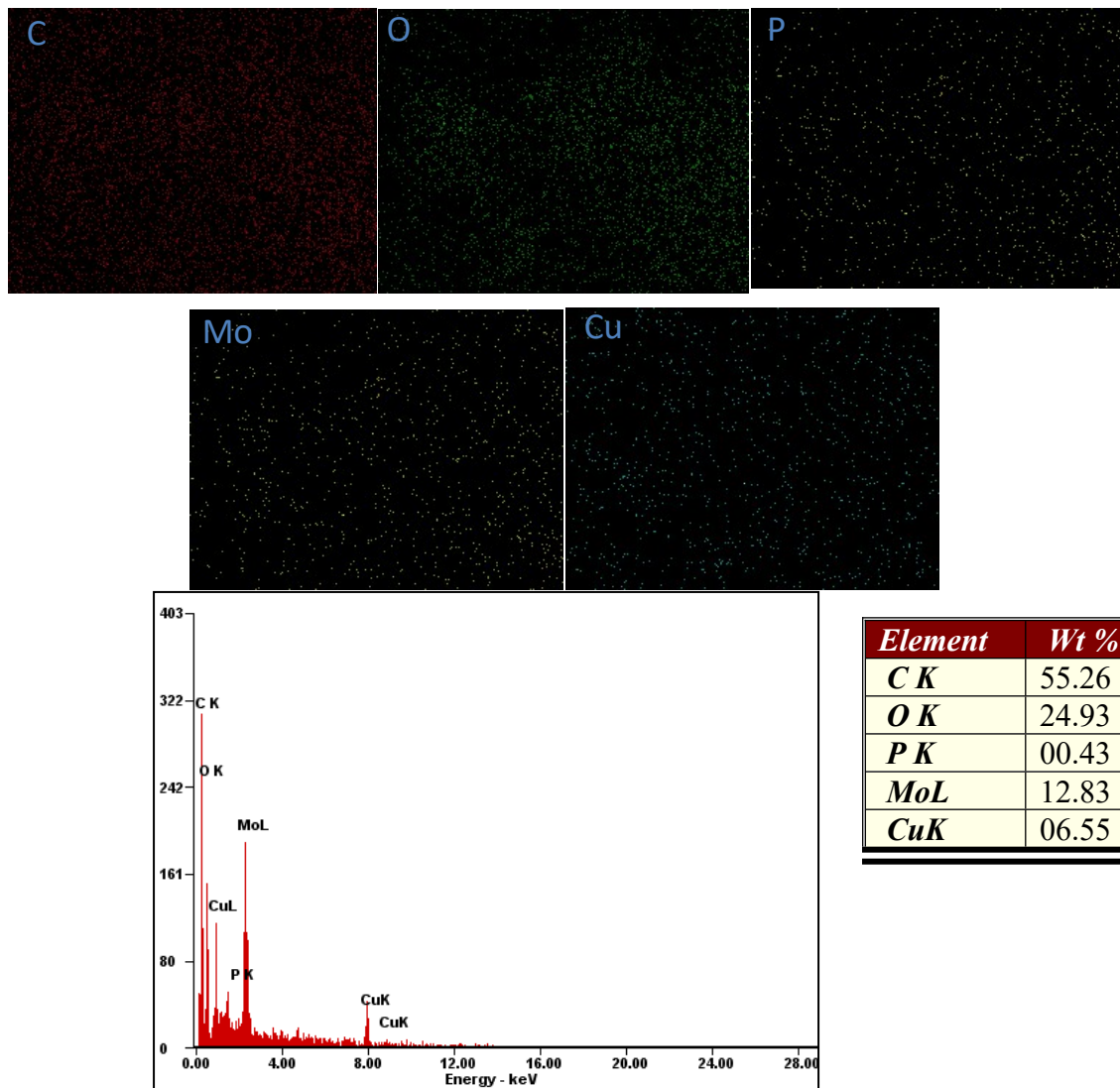
Fig. S1: SEM-EDS analysis of NENU-5 MOF
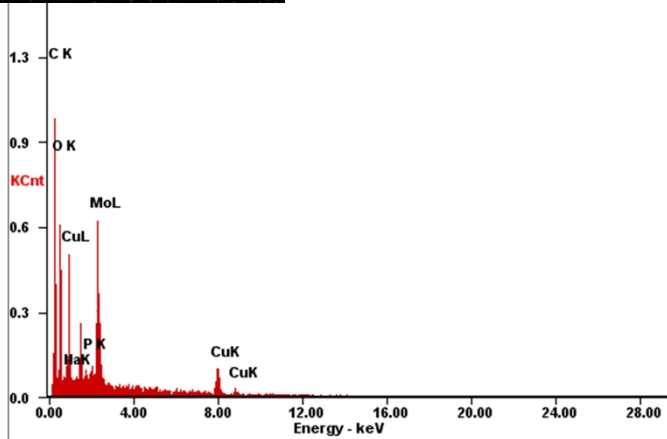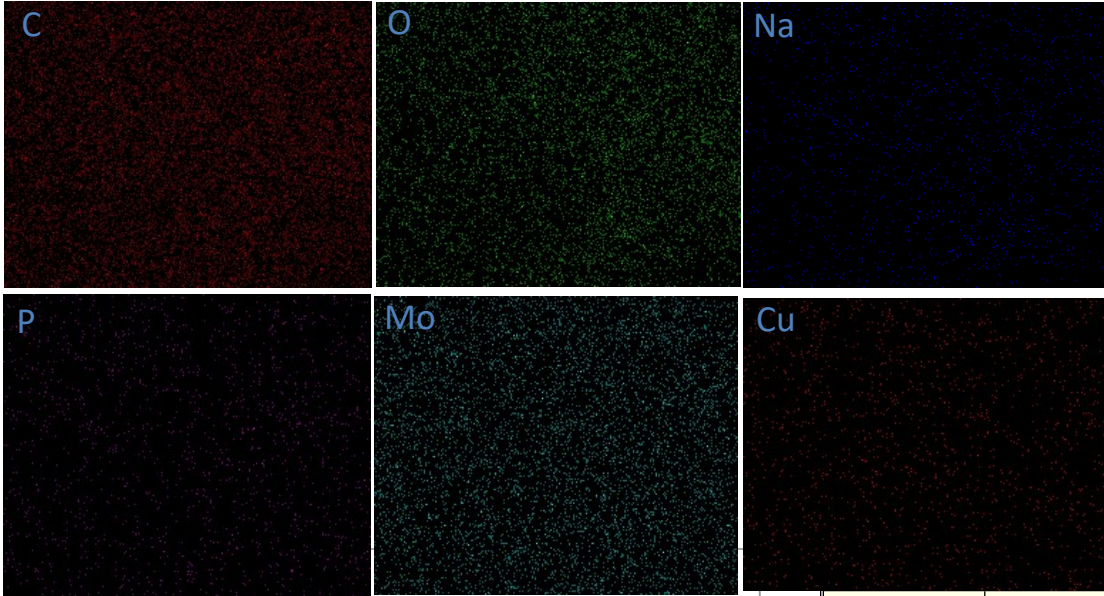
		At %
C K	56.50	71.92
O K	25.71	24.57
NaK	00.10	00.07
P K	00.26	00.13
MoL	10.78	01.72
CuK	06.63	01.59
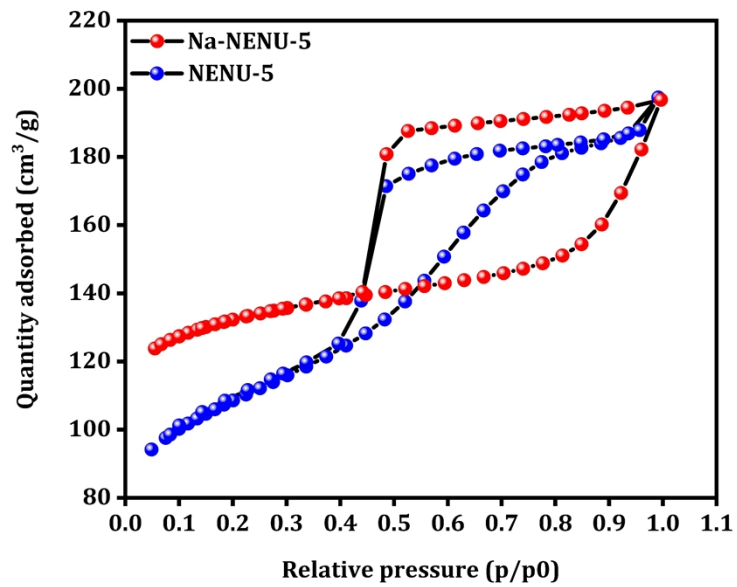
Fig. S3: N_2 adsorption-desorption isotherms of NENU-5 and Na-NENU-5

250nm

C Kα1_2

Mo Kα1

250nm

250nm

Cu Kα1

Na Kα1_2
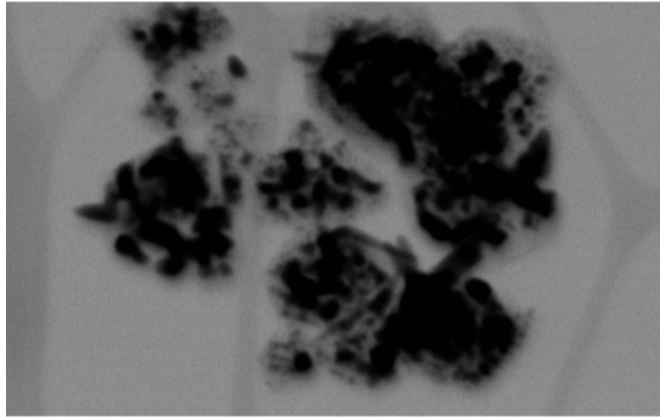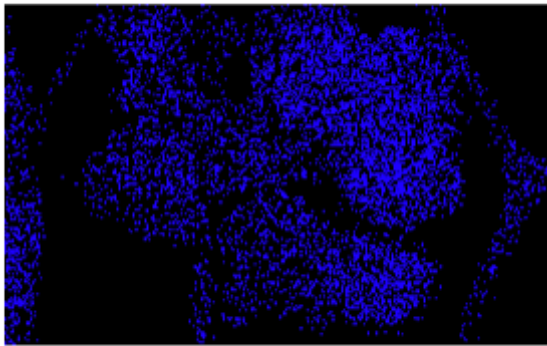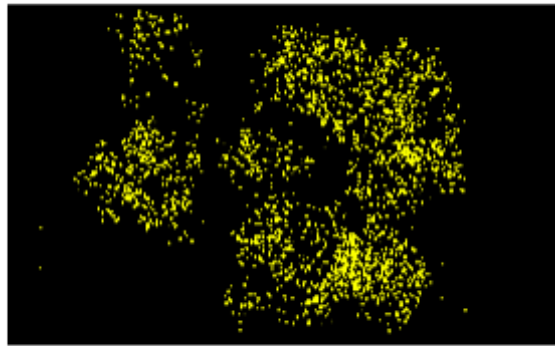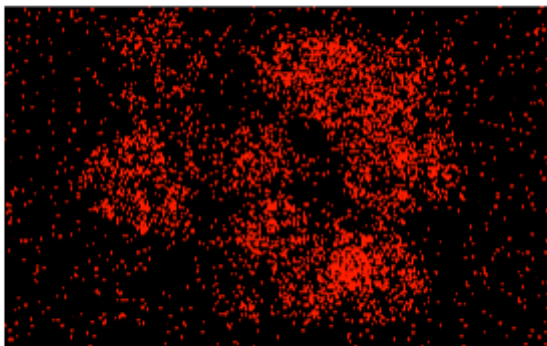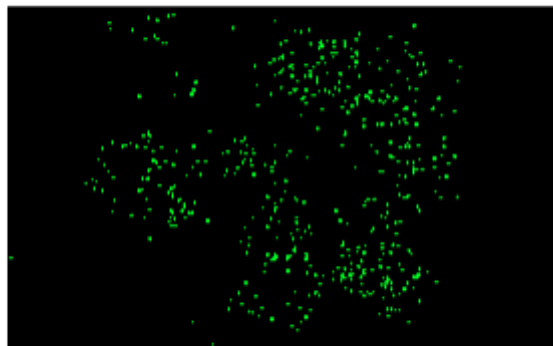
250nm

250nm

Fig. S4: TEM-EDS mapping of Na-Cu-Mo$_2$C
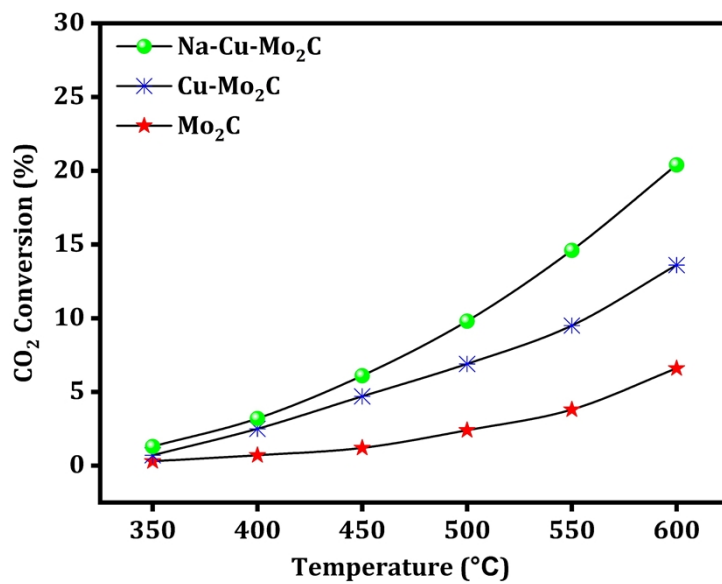
Fig. S5: RWGS activity of the derived catalysts (Enlarged portion of Fig. 8a)
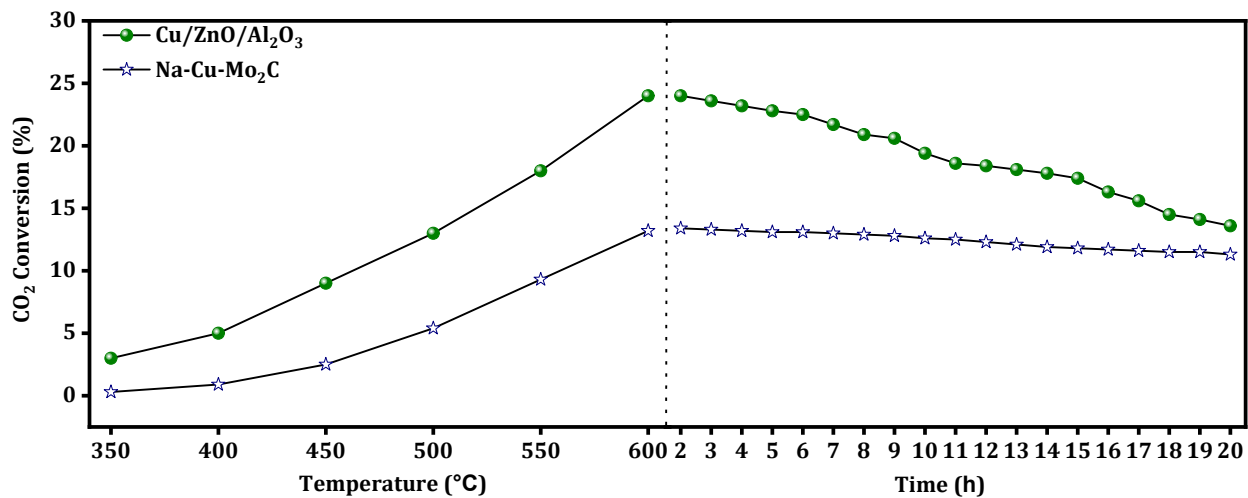
Fig. S6: Comparison of the Na-Cu-Mo$_2$C catalyst with benchmark Cu/ZnO/Al$_2$O$_3$ catalyst

Electron Image 1

500nm

C Kα1_2

500nm

Mo Kα1

500nm

Cu Kα1
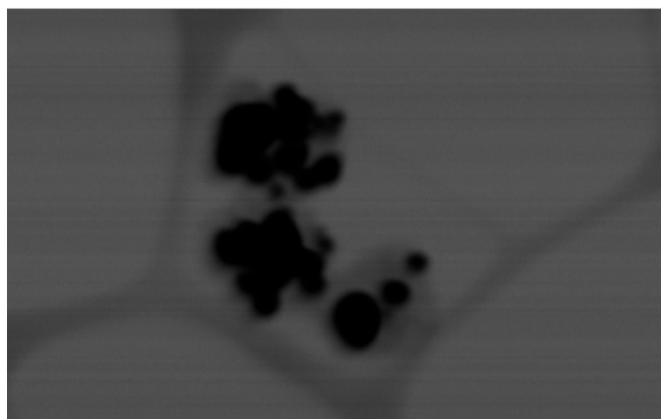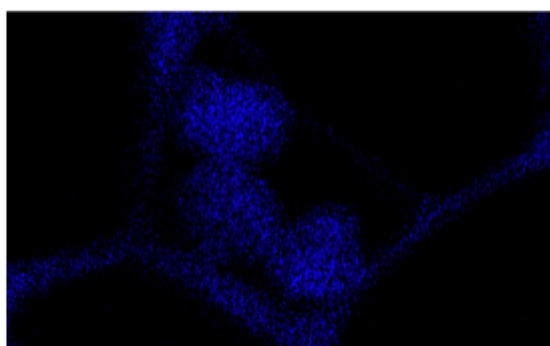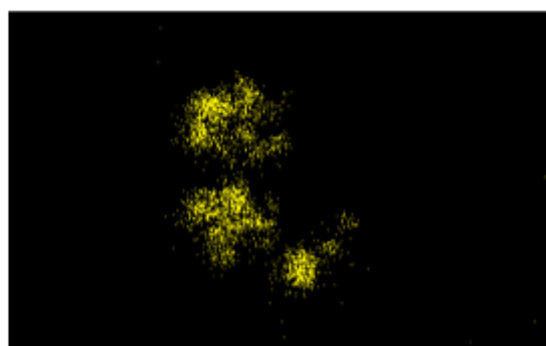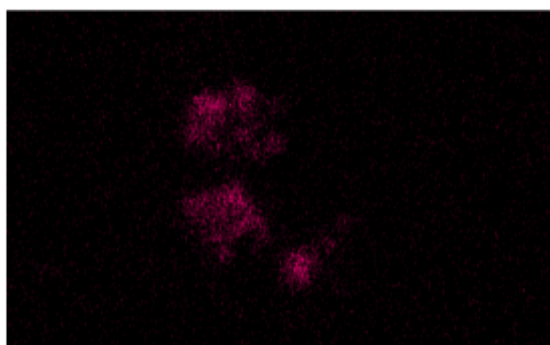
500nm

Na Kα1_2
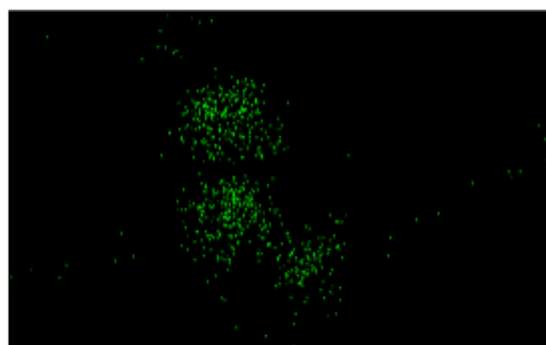
500nm

Fig. S7 TEM-EDS mapping after stability test for 100 h at 800 °C over Na-Cu-Mo$_2$C catalyst

Table S1: A detailed Comparison of the best-reported Fe, Co, and Cu-based catalysts for CO_2 to CO conversion with this work

Catalysts	$H_2:CO_2$ ratio	CO_2 Conversion (%)	Temperature (°C)	GHSV (mL g$^{-1}_{cat}$ h^{-1})	CO selectivity (%)	CO Yield (%)	CO production rate (mmol h^{-1} g$_{cat}^{-1}$)	H_2 Pre-treatment	Stability test (h)	Ref.
CuO/γ-Al$_2$O$_3$	4:1	60	600	60000	100	60	-	Yes	80	1
0.25Fe0.75Cu	4:1	37	450	60000	100	37	134.3	No	48	2
FeCu/CeAl	4:1	42	500	30000	100	42	102.2	Yes	48	3
DFNS-TiO$_2$-Cu10	1:1	10	600	2842000	99.8	9.98	5350	Yes	200	4
CuSiO-I	2:1	9.8	600	3000000	100	9.8	2585	Yes	45	5
Cu-2D-SiO$_2$-850r	2:1	10	550	3000000	100	10	296	Yes	54	6
K-Co/CeO$_2$ (1/10)	1:1	37	600	300000	100	37	2478	Yes	NR	7
15CuCe	3:1	60	600	400200	100	60	2466	Yes	230	8
Cu/Al$_2$O$_3$	2:1	47	600	300000	100	47	2097	Yes	40	9
Cu/β-Mo$_2$C	2:1	40	600	300000	100	40	1786	Yes	40	10
CuSiO/CuOx	3:1	17.8	500	60000	100	17.8	114	Yes	24	11
Cu/Al$_2$O$_3$	-	50	600	20000	100	50	22	Yes	NR	12
Co/Mo$_2$C	2:1	9.5	600	36000	100	9.5	51	Yes	36	13
Na-Cu-Mo$_2$C	**1:1**	**5.9**	**600**	**3000000**	**100**	**5.9**	**3230**	**No**	**250**	**This work**
Na-Cu-Mo$_2$C	**4:1**	**74**	**800**	**10000**	**100**	**74**	**57.8**	**No**	**100**	**This work**

References

1 A. Zakharova, M. W. Iqbal, E. Madadian and D. S. A. Simakov, *ACS Appl. Mater. Interfaces*, 2022, **14**, 22082–22094.

2 L. Yang, L. Pastor-Pérez, J. J. Villora-Pico, A. Sepúlveda-Escribano, F. Tian, M. Zhu, Y.-F. Han and T. Ramirez Reina, *ACS Sustainable Chem. Eng.*, 2021, **9**, 12155–12166.

3 L. Yang, L. Pastor-Pérez, J. J. Villora-Pico, S. Gu, A. Sepúlveda-Escribano and T. R. Reina, *Applied Catalysis A: General*, 2020, **593**, 117442.

4 R. Belgamwar, R. Verma, T. Das, S. Chakraborty, P. Sarawade and V. Polshettiwar, *J. Am. Chem. Soc.*, 2023, **145**, 8634–8646.

5 R. Jin, J. Easa and C. P. O'Brien, *ACS Appl. Mater. Interfaces*, 2021, **13**, 38213–38220.

6 S. Wang, K. Feng, D. Zhang, D. Yang, M. Xiao, C. Zhang, L. He, B. Yan, G. A. Ozin and W. Sun, *Advanced Science*, 2022, **9**, 2104972.

7 L. Wang, H. Liu, Y. Chen, R. Zhang and S. Yang, *Chem. Lett.*, 2013, **42**, 682–683.

8 H.-X. Liu, S.-Q. Li, W.-W. Wang, W.-Z. Yu, W.-J. Zhang, C. Ma and C.-J. Jia, *Nat Commun*, 2022, **13**, 867.

9 A. M. Bahmanpour, F. Héroguel, M. Kılıç, C. J. Baranowski, L. Artiglia, U. Röthlisberger, J. S. Luterbacher and O. Kröcher, *ACS Catal.*, 2019, **9**, 6243–6251.

10 X. Zhang, X. Zhu, L. Lin, S. Yao, M. Zhang, X. Liu, X. Wang, Y.-W. Li, C. Shi and D. Ma, *ACS Catal.*, 2017, **7**, 912–918.

11 Y. Yu, R. Jin, J. Easa, W. Lu, M. Yang, X. Liu, Y. Xing and Z. Shi, *Chem. Commun.*, 2019, **55**, 4178–4181.

12 S. Choi, B.-I. Sang, J. Hong, K. J. Yoon, J.-W. Son, J.-H. Lee, B.-K. Kim and H. Kim, *Sci Rep*, 2017, **7**, 41207.

13 M. D. Porosoff, X. Yang, J. A. Boscoboinik and J. G. Chen, *Angewandte Chemie International Edition*, 2014, **53**, 6705–6709.